



Journal of Colloid and Interface Science 278 (2004) 44-52

JOURNAL OF
Colloid and
Interface Science

www.elsevier.com/locate/jcis

# Characterization of DNA immobilization and subsequent hybridization using in situ quartz crystal microbalance, fluorescence spectroscopy, and surface plasmon resonance

Yoon-Kyoung Cho <sup>a,\*,1</sup>, Sunhee Kim <sup>a,1</sup>, Young A Kim <sup>a</sup>, Hee Kyun Lim <sup>a</sup>, Kyusang Lee <sup>a</sup>, DaeSung Yoon <sup>a</sup>, Geunbae Lim <sup>a,2</sup>, Y. Eugene Pak <sup>a</sup>, Tai Hwan Ha <sup>b</sup>, Kwan Kim <sup>b</sup>

a Digital Bio Laboratory, Samsung Advanced Institute of Technology, Suwon 440-600, South Korea
 b Laboratory of Intelligent Interface, School of Chemistry and Center for Molecular Catalysis, Seoul National University, Seoul 151-742, South Korea
 Received 23 June 2003; accepted 5 May 2004

Available online 2 July 2004

#### **Abstract**

We have characterized the immobilization of thiol-modified oligomers on Au surfaces and subsequent hybridization with a perfectly matched or single-base mismatched target using a quartz crystal microbalance (QCM) and fluorescence spectroscopy. The surface density of immobilized probe molecules and the hybridization efficiency depending on the type of buffer and salt concentration were investigated. We observed some ambiguities in surface coverage deduced from QCM measurement and adopted a complementary fluorescence displacement method. Direct comparison of surface coverage deduced from frequency change in QCM measurement and determined by the fluorescence exchange reaction revealed that QCM results are highly overestimated and the amount of overestimation strongly depends on the type of buffer and the structure of the film. Discrimination capability of the surface attached 15-mer probe was also examined using a single-base mismatched target at various hybridization temperatures. Hybridization efficiency depending on the type of single base mismatch was investigated using surface plasmon resonance (SPR).

© 2004 Published by Elsevier Inc.

### 1. Introduction

There is explosive interest regarding the use of DNA-functionalized surfaces to detect complementary target DNA sequences in a complex DNA mixture by using the high specificity inherent in DNA base pairing. The applications include genetic and infectious disease diagnostic devices [1,2], miniaturized biosensor arrays [3], and DNA-driven assembly of nanostructures [4–7].

The interaction between probes, surface-tethered singlestranded DNA, and the complementary target DNA strands in solution plays the most crucial role in these applications. Therefore it is important to have a good understanding of the key factors influencing the efficiency and selectivity of these molecular recognition events. Among many strategies for immobilizing DNA probes on surfaces, thiol-modified DNA probes that are immobilized on Au surfaces through self-assembly have been employed by several researchers as a model system to obtain better physical insights into the ability of DNA monolayers to capture and discriminate complementary and noncomplementary target sequences in free solution [8–13].

Tarlov and co-workers estimated the surface coverage of surface-bound DNA molecules and their structure under various conditions using a number of surface analysis techniques, such as X-ray photoelectron spectroscopy (XPS), ellipsometry, radiolabeling, electrochemistry, and neutron reflectivity [8,9,11]. They could control the surface coverage and thus maximize the hybridization efficiency by treating oligonucleotide-modified surfaces with small space-blocking molecules, 6-mercapto-1-hexanol (MCH). When

<sup>\*</sup> Corresponding author. Fax: 82-31-280-8277. E-mail address: dnachip@samsung.com (Y.-K. Cho).

<sup>&</sup>lt;sup>1</sup> The authors wish it to be known that, in their opinion, the first two authors should be regarded as joint first authors.

<sup>&</sup>lt;sup>2</sup> Current address: Department of Mechanical Engineering, Pohang University of Science and Technology, San 31 Hyoja-dong, Nam-gu, Pohang, Kyungbuk 790-784, South Korea.

the surface is passivated by MCH, it not only prevents nonspecific adsorption of target DNA in solution, but also displaces weakly adsorbed DNA strands on the substrate, leaving single-stranded probe DNA with a more extended conformation and thus facilitating hybridization.

In addition, a recent study reported an increase of hybridization efficiency as well as a higher surface density when a mixed self-assembled monolayer (SAM) of HS-ss-DNA/alkanethiol was employed. The mixed SAM of HS-ss-DNA/alkanethiol were prepared by sequential adsorption of HS-ss-DNA on a freshly exposed gold surface that was previously covered by short alkanethiols and later selectively desorbed from mixed length alkanethiols [14].

While most of the previous studies using surfaces tethered with thiol-modified oligonucleotide probes focused on hybridization with oligonucleotide targets, Huang et al. investigated hybridization with much longer polynucleotide targets using atomic force microscopy (AFM) and a quartz crystal microbalance (QCM) [15].

The morphology of self-assembled DNA films was also investigated using scanning probe microscopy (SPM) [16]. It was observed that the film structure was significantly affected by a small change such as modifying the position of the thiol group from the 5' end to the 3' end of DNA [16].

The kinetic characteristics of the immobilization of the thiol-modified DNA and subsequent hybridization with a complementary oligonucleotide target have been studied using surface plasmon resonance (SPR) spectroscopy [17–19]. It was found that the kinetics of self-assembly of thiol-modified ss-DNA has to take desorption and diffusion into account, in addition to adsorption. It was also reported that the rate of hybridization depends not only on the degree of mismatch but also on the position at which the hybridization occurs along the immobilized probe strands [19].

The QCM method has been adopted by several groups to detect the DNA hybridization reaction because of its great sensitivity as a mass sensor capable of measuring subnanogram mass changes. It also has the great advantage of not requiring post-treatment of target samples, such as fluorophore or radioisotope labeling, for detection [20–27]. Okahata et al. conducted a systematic study to compare the kinetic parameters under various experimental conditions using 27-MHz QCM [24]. Hook et al. monitored the immobilization of PNA or DNA and studied the hybridization with DNA using a QCM dissipation monitoring technique [27]. To employ QCM as a DNA hybridization sensor, a number of studies reported techniques to enhance the sensitivity of QCM detection. QCM crystals of higher frequency can increase the sensitivity even though a highfrequency (> ~10-MHz) device may show unstable frequency response when operated in aqueous solutions [22]. The sensitivity could be also improved by increasing the hybridization capacity using self-assembled DNA films [14], multilayers of DNA films [22], or DNA dendrimers [26] as probe surfaces. Additionally, the hybridization signal could be amplified by increasing the total mass by derivatizing the target DNA with liposomes [21] or gold nanoparticles [28,29].

So far, there have been a few reports using thiolated DNA-modified surfaces to understand the relationship between surface coverage, structure, and hybridization efficiencies and thus to provide better physical insights into the development of new DNA detection methods. However, key factors influencing the probe density and hybridization efficiency are still far from full elucidation.

Herein we described the experimental methods for characterizing hybridization of thiol-modified 15-mer DNA probes with perfectly matched and single-base mismatched target molecules. Effects of the type and concentration of buffer on immobilized probe density and hybridization efficiency were explored. We observed that there were some ambiguities in surface coverage deduced from QCM measurements, depending on the type of buffer used. In order to quantitatively determine the surface coverage, we adopted a new complementary fluorescence-based method. A direct comparison of surface coverage deduced from frequency change and fluorescence measurement was made for the first time, to the best of our knowledge. The surface coverage determined by fluorescence-based methods revealed that the surface density estimated by QCM measurements was highly overestimated and the amount of overestimation strongly depended on the type of buffer as well as the structure of the film. We demonstrated that a fluorescencebased surface-coverage-detection method can be useful as a complementary technique to semiquantitative QCM measurement. In addition, the temperature dependence on the amount of nonspecific adsorption during hybridization with a single-base mismatched target was investigated using QCM. Finally, SPR was utilized to investigate the effect of the type of mismatch on the hybridization efficiency.

## 2. Materials and methods

#### 2.1. Chemicals

Tris(hydroxymethyl)aminomethane hydrochloride (Tris-HCl), ethylenediaminetetraacetic acid (EDTA), mercaptohexanol (HS(CH<sub>2</sub>)<sub>6</sub>OH), 3-mercaptopropanol (MPA), NaH<sub>2</sub>PO<sub>4</sub>, and NaOH were purchased from Aldrich and used as received. All oligonucleotides were purchased from Genotech (Daejeon, Korea). Sequences are as given in Table 1. The sequences were chosen because they are believed to be a part of the iduronate-2-sulfate (IDS) coding region, whose mutation is suspected to be one of the main causes of Hunter syndrome.

#### 2.2. QCM crystals and instrumentation

The QCM crystals used were 10-MHz AT-cut crystals (International Crystal Manufacturing Co. Inc., OK). The quartz crystal was mounted onto a QCM cell, made of Teflon, and 30 ml of the buffer solution was introduced. The

Table 1 Nomenclatures and sequences of oligonucleotides

Name	Sequence (5' to 3')
Probe	HS(CH <sub>2</sub> ) <sub>6</sub> -5'-GTTCTTCTCATCATC-3'
F-Probe	HS(CH <sub>2</sub> ) <sub>6</sub> -5'-GTTCTTCTCATCATC-3'-Fluorescein
B-Probe	5'-Biotin-GTTCTTCTCATCATC-3'
TA-PM-Target	3'-CAAGAAG <u>A</u> GTAGTAG-5'
TT-SPM-Target	3'-CAAGAAG <u>T</u> GTAGTAG-5'
TG-SPM-Target	3'-CAAGAAGGGTAGTAG-5'
TC-SPM-Target	3'-CAAGAAGCGTAGTAG-5'
D-Target	3'-GCAAGAATAGTAGCA-5'

solution was agitated with a small magnetic stirrer throughout the measurement. The experimental setup allows temperatures in the range 15–60 °C. The QCM cell was designed so that only one gold-coated side of the quartz disk was in contact with the solution. A detailed description is given elsewhere [30].

The measured frequency change in QCM experiments,  $\Delta F$  (Hz), is approximately related to the mass change by adsorption,  $\Delta m$  (g), on the quartz crystal by the Sauerbrey equation,

$$\Delta F = -\frac{2F_0^2 \Delta m}{A\sqrt{\mu_{\rm q}\rho_{\rm q}}},\tag{1}$$

where  $F_0$  is the fundamental frequency of the QCM (10 MHz), A is the electrode area (0.2 cm<sup>2</sup>),  $\mu_q$  is the shear modulus of quartz (2.947 × 10<sup>11</sup> dyn cm<sup>-2</sup>), and  $\rho_q$  is the density of quartz (2.648 g cm<sup>-3</sup>). The frequency change of 1 Hz corresponds to a mass change of 0.883 ng.

#### 2.3. Procedure of immobilization and hybridization

The experimental scheme is as sketched in Fig. 1. A bare Au electrode on a quartz crystal was cleaned with piranha solution (3:1 H<sub>2</sub>SO<sub>4</sub>:30% H<sub>2</sub>O<sub>2</sub>). (Note: This is a dangerous cleaning solution and care must be taken in solution handling.) After thorough rinsing with H<sub>2</sub>O, the quartz crystal was mounted on the QCM cell, aqueous buffer solution was introduced, and the temperature was set to 23 °C. Once a stable frequency baseline was established, probe solution with a concentration of 0.58 µM in 1 M PBS (1 M NaH<sub>2</sub>PO<sub>4</sub> at pH 5.7) or in TE-1 M NaCl (10 mM Tris-HCl, 1 mM EDTA, 1 M NaCl, pH 7.6) was injected and the frequency decrease was monitored until it reached an equilibrium value. The concentration of the probe solution was chosen based on the literature [11], which used 0.5–1 µM. Our preliminary experiments showed there was no significant difference when we used 0.2–1 μM of the probe solution. To reduce nonspecific adsorption of target DNA and enhance the degree of hybridization, 1 mM mercaptohexanol, HS(CH<sub>2</sub>)<sub>6</sub>OH, was introduced after the QCM cell was cleaned with buffer and rinsed with deionized water. The QCM cell was filled with TE-1 M NaCl buffer and the target oligomer was injected to be 0.58 µM; we then waited until a stable baseline was obtained. Finally this setup was rinsed with TE-1 M NaCl,

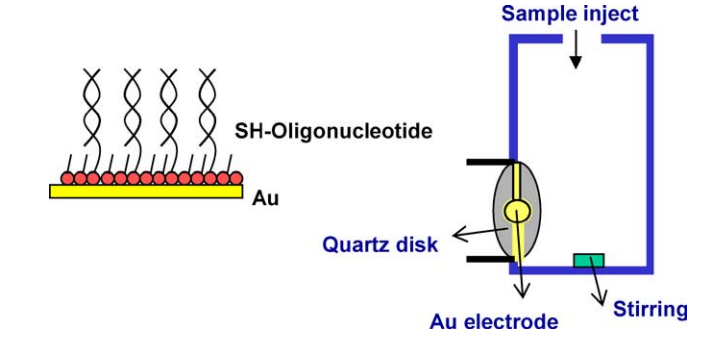


Fig. 1. Schematic diagram of thiol-modified oligonucleotides on QCM crystals and the experimental setup for QCM measurements of DNA immobilization and hybridization. Only one face of the quartz disk is faced on the liquid.

followed by a deionized water rinse. Frequency response was reset to zero after stabilization each time the liquid was exchanged.

# 2.4. Quantification of surface density and hybridization efficiency

Gold thin film was prepared on slide glasses (2.3  $\times$ 3.8 cm) using the same method as was used to prepare the gold layer on QCM crystals was prepared. A 1-nm-thick adhesive layer of Cr was sputtered on glass surfaces, followed by sputtering of 500 nm of Au. A close examination using AFM study showed little difference between the prepared Au thin-film surface on glasses and QCM crystals. The surface of the gold thin film was cleaned with piranha solution and then rinsed several times with deionized water. The method of quantification method of oligonucleotides immobilized on gold surfaces followed that of a previous report [31]. Fig. 2 summarizes the schematics of our experimental procedure. A fluorescence-attached DNA probe (shown as the F-probe in Table 1) immobilized on a gold substrate was placed in 20 mM 3-mercaptopropanol in TE buffer solution at room temperature for 20 h, which was a sufficient concentration and time to reach the equilibrium of the replacement reaction of the adsorbed species and 3-mercaptopropanol. The fluorescein-labeled oligonucleotides desorbed from the gold surface were collected with a washing solution and the fluorescent signal of the solution was measured and converted to surface coverage using the standard curve previously prepared. The fluorescence intensity was measured at 520 nm using an FP 750 fluorometer (JASCO).

## 3. Results and discussion

## 3.1. Direct monitoring of DNA immobilization and hybridization

QCM was utilized for in situ monitoring and quantification of immobilized probe oligonucleotide on Au surface

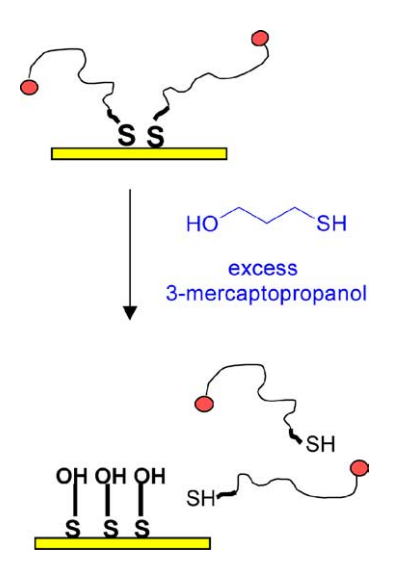


Fig. 2. Schematic diagram of quantification of surface coverage by displacement of F-Probe adsorbed on Au surfaces using 3-mercaptopropanol.

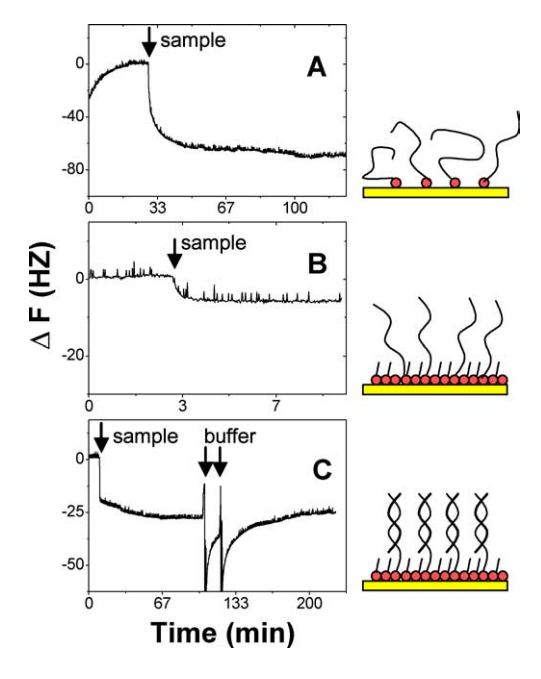


Fig. 3. Typical time dependence of frequency decrease of QCM upon introduction of (A) 0.58  $\mu$ M probe DNA in 1 M PBS, (B) 1 mM mercaptohexanol, (C) 0.58  $\mu$ M target DNA in TE–1 M NaCl. Arrows indicate the time when the sample was injected. The second and third arrows in (C) indicate the times when the buffer solution was introduced to wash out nonspecifically adsorbed molecules. Immobilization and adsorption of mercaptohexanol were done at 25 °C and the hybridization was done at 38 °C.

and subsequent hybridization with target molecules. Fig. 3 shows a typical time course of frequency change upon the introduction of 0.58  $\mu$ M probe DNA (Fig. 3A), 1 mM mercaptohexanol (Fig. 3B), and 0.58  $\mu$ M target DNA (Fig. 3C). Arrows in the figure indicate the times when the sample and rinsing buffer solutions were injected. CV% in frequency drop in QCM measurements was about 10–15% depending on the conditions. Fig. 3 is a typical example of the time course of the reaction and the calculation of the sur-

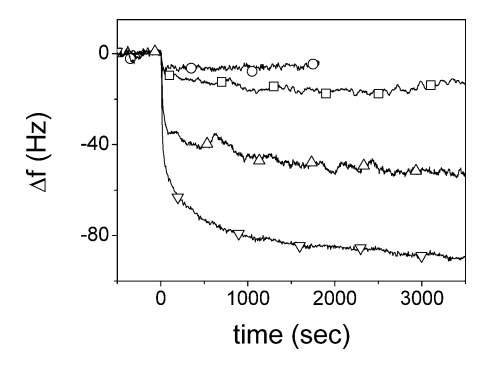


Fig. 4. Frequency changes responding to the addition of  $0.58~\mu M$  probe oligonucleotides in 1 M PBS (down triangles), 0.2~M PBS (up triangles), 0.01~M PBS (squares), and DI water (circles).

face coverage based on frequency drop was done using three independent experimental data.

In Fig. 3A, the concentration of the probe DNA (Probe) was 0.58  $\mu M$  in 1 M PBS and a frequency drop of 80 Hz was observed. Assuming the Sauerbrey equation and a sensitivity of 0.883 ng/Hz, the surface coverage was calculated to be  $4.7 \times 10^{13}$  molec/cm². The first drop of frequency occurs as the adsorption of thiol-attached probe DNA begins, followed by slow rearrangement, which has been also observed previously and reported as a characteristic of thiol adsorption on gold surfaces [32].

In Fig. 3B, the frequency decrease responding to the addition of 1 mM mercaptohexanol, HS(CH<sub>2</sub>)<sub>6</sub>OH, is shown. Mercaptohexanol was used because it is known that it can impede nonspecific adsorption of target DNA and enhance the hybridization reaction [8,33]. Additional adsorption of mercaptohexanol gave a frequency drop of as much as 8 Hz, which corresponds to an additional adsorbed mass of 3.1 × 10<sup>14</sup> molec/cm<sup>2</sup>. Levicky et al. reported that hybridization efficiency was less than 10% without the postadsorption of mercaptohexanol [11]. Our preliminary experiments showed that hybridization efficiency was increased up to 30% by using postadsorption of mercaptohexanol.

Fig. 3C shows the frequency response when 0.58- $\mu$ M target oligomer solution in TE–1 M NaCl was introduced. The last two arrows denote the time when TE–1 M NaCl buffer was injected to rinse out nonspecifically adsorbed molecules. After rinsing with buffer twice, the frequency drop was stabilized at about 25 Hz. Assuming the Sauerbrey equation, additional mass increase was 1.5  $\times$  10<sup>13</sup> molec/cm² and therefore it is estimated that 31% of probe molecules participated in the hybridization.

In order to investigate the effects of ionic strength on the immobilized probe density, frequency drop upon injection of probe solution at various concentrations of phosphate solution was measured. As shown in Fig. 4, the frequency drop due to probe immobilization gradually increased as the concentration of phosphate solution increased. By simple estimation from frequency drop, the surface density of the probe DNA was  $4.7 \times 10^{13}$  molec/cm<sup>2</sup> (~frequency drop of 80 Hz) when 1.0 M PBS was used, while it was

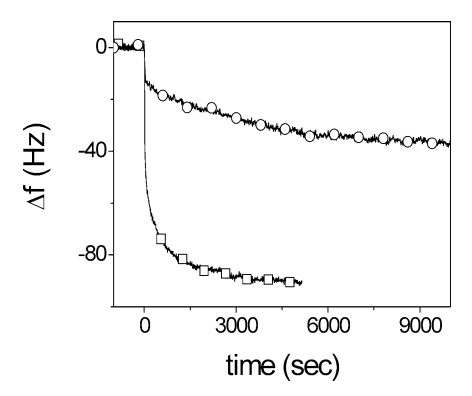


Fig. 5. Frequency responses upon addition of 0.58  $\mu M$  probe oligonucleotides in 1 M PBS (squares) and TE-1 M NaCl (circles).

 $9.3 \times 10^{12}$  molec/cm<sup>2</sup> (~frequency drop of 16 Hz) when 0.01 M PBS was used. The increase of surface density at higher concentrations of phosphate solution can be explained by the decrease of electrostatic repulsion between anionic DNA chains.

The surface coverage of close-packed ss-DNA strands can be simply estimated as  $6 \times 10^{13}$  to  $9 \times 10^{13}$  molec/cm² from the assumption of 0.6 to 0.7 nm of cross-sectional radius of each ss-DNA chain [10]. This simple calculation tends to be overestimated, since it does not take into account the electrostatic repulsion and steric hindrance effects of the surrounding counterions and hydrating water molecules. Surface density of thiol-modified ss-DNA on Au surface varies with measurement techniques as well as the immobilization conditions and the length of the oligonucleotides. Nonetheless, the measured probe density of  $4.7 \times 10^{13}$  molec/cm² when 1 M PBS was used seems to be highly overestimated compared to the estimated maximum of  $6 \times 10^{13}$  to  $9 \times 10^{13}$  molec/cm².

Frequency drops upon DNA probe immobilization when two different types of buffer were used are compared in Fig. 5. When TE-1 M NaCl instead of 1 M PBS was used, the frequency drop was only 36 Hz, compared to 80 HZ for 1.0 M PBS. Furthermore, the adsorption was much slower. We expected to obtain similar results from two different types of buffers because the ionic strengths of the buffers are similar. This nonintuitive result led us to the next topic, the quantification of surface coverage using fluorescence measurements, described in Section 3.2.

# 3.2. Quantification of surface coverage and hybridization efficiency

As discussed in Section 3.1, QCM measurement suggested about two times larger probe density when 1 M PBS instead of TE-1 M NaCl was used as an immobilization buffer. The salt concentration and other experimental conditions were similar. In order to dissolve this ambiguity, we adopted a separate surface coverage measurement technique, a fluorescence-based method originally suggested by Demers et al. [31] for thiol-modified oligomers immobilized

Table 2
Comparison of the surface density measured by QCM and fluorescence-based method

Immobilization	QCM: $\Delta f$ (Hz)	Probe density (×10 <sup>12</sup> molec/cm <sup>2</sup> )		
buffer		QCM	Fluorescence	
TE-1 M NaCl	36	20.9	4.3	
1 M PBS	80	46.5	4.0	
0.2 M PBS	51	29.7	1.2	
0.01 M PBS	16	9.3	0.3	
DI water	6	3.5	0.1	

on gold nanoparticles. This technique is based on the displacement of fluorescence-tagged probe molecules by small alkanethiol molecules, 3-mercaptopropanol (MPA). The detailed experimental technique is described in the Experimental section. Direct measurement of the fluorescent intensity of fluoropore tethered on metal surfaces was not accurate because of the fluorescence quenching effect.

Probe densities estimated from QCM measurements and fluorescence-based methods were compared in Table 2. The data were the average of three independent measurements. Increase of the surface density as the salt concentration was increased is not surprising. However, in contrast to the QCM measurements, fluorescence measurements showed that the surface densities did not depend on the type of buffer, TE–1 M NaCl or 1 M PBS. Moreover, the surface coverage measured by the QCM technique was highly overestimated. The surface density estimated by QCM frequency change was about 5 times larger than the density measured by the fluorescence-based method for TE–1 M NaCl and 10 times larger for 1 M PBS.

The overestimation of the QCM experiments were also reported using X-ray photoelectron spectroscopy with polyelectrolytes with different charge density [34]. The overestimation of the adsorbed mass from QCM measurements was a factor of 4.4 higher than that measured using XPS for low-charged polyelectrolytes, while it was about the same for highly charged polyelectrolytes. This is possibly due to the difference in the structure of the adsorbed layer. If the adsorbed layer has a conformation such that structure is more extended and nonrigid, the overestimation could be higher because of the contribution from the hydrodynamically coupled buffer within the layer.

Based on our experimental observations, the overestimation was higher for the PBS buffer. One possible cause for the overestimation could be that the difference in pH (pH 5.7 for PBS, pH 7.6 for TE) could produce conformational differences in adsorbed probes even though the salt concentration was high, 1 M. At low pH, the adsorbed probes could be more balanced in charge and apparently could have more extended and less rigid conformation. In addition, the viscoelastic properties of the adsorbed layer due to the conformational differences of the layer and also due to the differences in densities or viscosities of the buffer could bring about the differences in overestimation. Investigation of conformation and viscoelastic properties using a surface forces

Table 3					
Hybridization	efficiency	measured b	y fluoresce	nce-based	method

Immobilization buffer	Probe density (×10 <sup>12</sup> molec/cm <sup>2</sup> )	Hybridization buffer	Hybridized DNA density (×10 <sup>12</sup> molec/cm <sup>2</sup> )	Hybridization efficiency (%)
TE-1 M NaCl	4.3	TE-1 M NaCl	2.6	60
1 M PBS	4.0	1 M PBS	3.1	75
		TE-1 M NaCl	2.6	65
		TE-0.2 M NaCl	1.1	28
		TE-0.01 M NaCl	0.5	13
		DI water	0.1	3

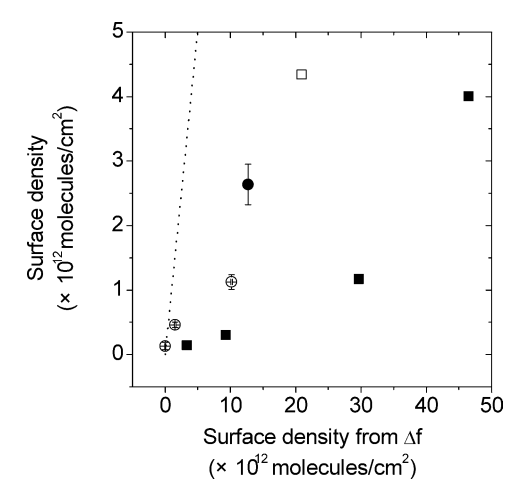


Fig. 6. Surface density measured by fluorescence-based method vs that estimated from frequency drop of QCM measurements. For ss-DNA molecules (squares), the surface coverage estimated from frequency change was more than 10 times overestimated for 1 M PBS buffer (closed squares). The overestimation was smaller for TE–1 M NaCl buffer (open squares). For hybridized DNA (circles), the overestimation was less than for single-stranded DNA. Hybridization buffers were TE–1 M NaCl (open circles) and 1 M PBS (closed circle). Dashed line indicates that the surface densities measured by two independent methods are the same. The overestimation of QCM measurement was smaller for the double-stranded DNA.

apparatus as we did previously [33] or QCM study with dissipation factor analysis would be more useful to study this phenomena.

Fluorescent displacement measurement was once more utilized to quantitate the hybridization efficiency. Hybridized double-stranded DNA tethered on an Au surface was replaced by MPA and the fluorescent concentration of the solution was measured. The results are summarized in Table 3. As one can expect, the hybridization efficiency was strongly affected by the salt concentration and little by the type of the buffer.

Fig. 6 shows the comparison of surface coverage estimated by a fluorescence-based method and by direct deduction from the frequency drop in QCM measurements. It is worthwhile to note that the overestimation was smaller for double-stranded DNA than for single-stranded probe DNA. This may imply that the structure of double-stranded DNA film is more rigid and therefore less water is bound compared to relatively flexible and bulky single-stranded DNA.

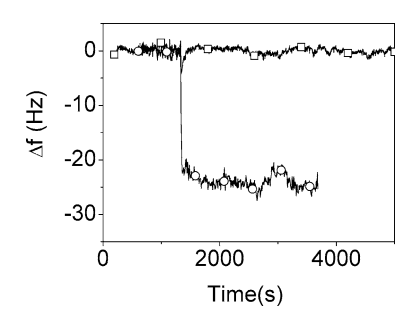


Fig. 7. Frequency responses when perfectly matched target (circles) and single-base mismatched target (squares) were introduced. Temperature was at  $38\,^{\circ}\text{C}$ .

In conclusion, quantitative measurement of surface density was accomplished as we introduced fluorescent-based displacement technique. In situ monitoring of the surface reaction was possible using QCM measurements, while quantitative information on the final surface coverage was obtained using a complementary fluorescence displacement technique.

# 3.3. QCM study of hybridization with single-base mismatched target

In order to investigate the possibility of nonspecific adsorption, hybridization experiments with single-base mismatched targets (TC–SPM-target in Table 1) were conducted. The melting temperature,  $T_{\rm M}$ , of probes hybridized with a perfectly matched sequence was predicted to be 58 °C using the nearest-neighbor model [35]. The  $T_{\rm M}$  of the oligomer hybridized with a single-base mismatched target (TC–SPM) was 48 °C. As shown in Fig. 7, there was hardly any change when the single-base mismatched target was introduced, while 25 Hz of frequency drop was observed when the perfectly matched target was used. The hybridization was done at 38 °C.

One can expect that the amount of hybridization would increase as the hybridization temperature decreased, while the selectivity with which the probe can discriminate perfectly matched and single-base mismatched sequences would decrease due to increased nonspecific hybridization. In order to decide the optimum hybridization temperature at which the hybridization signal is large enough to detect while the discrimination capability is not lost, we conducted a series of hybridization experiments at various tempera-

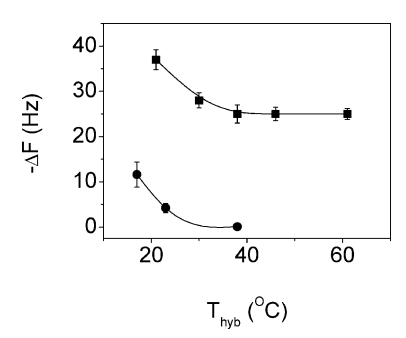


Fig. 8. Frequency responses upon hybridization with perfectly matched targets (squares) and single-base mismatched targets (circles) at various temperatures.

tures. The result is shown in Fig. 8. The nonspecific hybridization increased under the hybridization temperature at  $38\,^{\circ}$ C, whereas the amount of hybridization did not decrease significantly above  $38\,^{\circ}$ C.

## 3.4. SPR study of hybridization with various kinds of single-base mismatched target

A Biacore 3000 instrument (Biacore AB) was utilized to investigate the hybridization efficiency, depending on the type of base pair mismatch. SA-5 sensor chips (research grade, precoated with approximately 4000 RU streptavidin) and HBS buffer (10 mM HEPES pH 7.4, 0.15 M NaCl, 3.4 mM EDTA, 0.005% Surfactant P20) were purchased from Biacore AB. The SA chip has four independent fluid channels (FC). The detailed optical configuration is shown elsewhere [36]. All experiments were done at 38  $^{\circ}\text{C}$  and the flow rate was 30  $\mu\text{l}/\text{min}$ . The HBS buffer was adjusted to have 0.5 M NaCl and used as a running buffer.

The bare chip was first washed three times with a 1 M NaCl + 50 mM NaOH solution before each experiment to remove any residual noncovalently bound streptavidin. For probe immobilization, 30 µl of probe solution with a concentration of 100 fmol/µl was introduced to FC2 of the sensor chip surface. We used the bare chip surfaces, streptavidin (FC1), as a reference to calibrate any nonspecific bindings. A signal change of 581 RU was monitored for immobilized probes. Since 1000 RU (Resonance Unit) corresponds to approximately 1 ng/mm<sup>2</sup> and the area of the fluid channel is 1.2 mm<sup>2</sup>, the adsorbed amount is about 0.7 ng, corresponding to 149 fmol. When we repeated the experiments, the CV% of the adsorbed amount (RU) was less than 0.5%. Meanwhile, the maximum adsorbed amount, 707 RU, was obtained when we introduced 330 µl of probe solution, which corresponded to 182 fmol,  $9 \times 10^{12}$  molec/cm<sup>2</sup>.

After probe immobilization was done, 45  $\mu$ l of the running buffer was introduced to wash out the nonspecific binding. For each hybridization experiment, 45  $\mu$ l of each target solution with concentrations of 100, 50, 25, and 12.5 fmol/ $\mu$ l, respectively, was injected and then 45  $\mu$ l of running buffer was flowed to rinse possible nonspecific bindings.

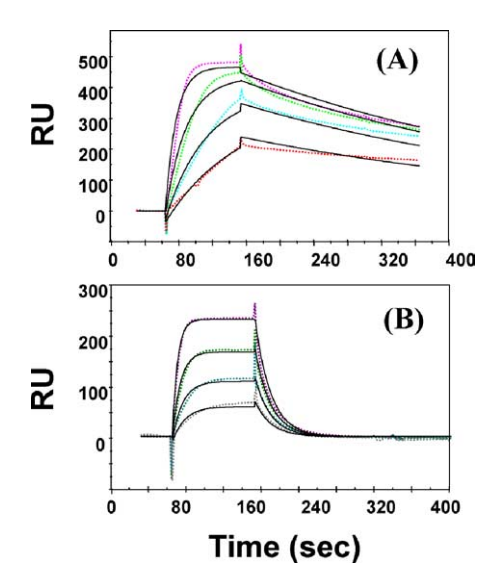


Fig. 9. Hybridization kinetics with perfectly matched target (Panel A: TA–PM-target) and single-base-pair mismatched target (Panel B: TT–SPM-target) were compared. A slower dissociation constant was observed for the perfectly matched target. A sample of 45 µl of target solution with a concentration of 100, 50, 25, or 12.5 fmol/µl from top to bottom lines, respectively, was introduced on the SA-5 chip immobilized with probe DNA. Broken lines are for fitted data for the analysis of the kinetic constant.

Table 4 SPR binding kinetics data

Targets	$K_{\rm a}(1/{ m Ms})$	$K_{\rm d}$ (1/s)	$K_{\rm A} \; ((1/{\rm M}) \times 10^4)$
TA-PM	754	0.00236	32
TG-SPM	1200	0.0595	2.0
TT-SPM	1290	0.0208	6.2

Fig. 9 shows the real-time monitoring data for hybridization with perfectly matched target (Panel A: TA–PM-target) and single-base mismatched target (Panel B: TT–SPM-target). For kinetic analysis, experiments with different target concentration were done. The kinetic constants were evaluated and are summarized in Table 4. As expected, the binding amount at equilibrium is higher when a higher concentration of target was introduced. Binding affinity for perfect matched hybridization (T–A binding) was about five times higher than that of T–T mismatched binding and 15 times higher for T–G mismatched binding. For other kinds of mismatches, T–C and deletion mutations, the binding amount were too small to evaluate kinetic data.

In Fig. 10, the binding data with different mutation types were compared. As expected, the perfectly matched target, T–A, showed the highest binding affinity; T–G and T–T mismatch showed some binding affinities, while T–C and deletion mutation showed smallest binding affinity. This tendency may be due to the stability of the mismatched duplexes and SPR is sensitive enough to distinguish these types of single-base mismatched duplexes. The results shown in Fig. 10 is very consistent with the prediction from the nearest neighbors model. The melting temperature predicted by the nearest neighbor model was 58, 53, 50, and 48 °C for

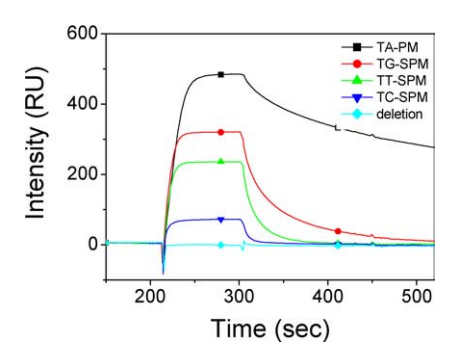


Fig. 10. Real-time monitoring of the hybridization with perfectly matched target (T–A: squares), single-base mismatched targets (T–G: circles; T–T: up triangles; T–C: down triangles), and (deletion mutation: diamond). Not only was the hybridization efficiency different, but also very distinctive differences in dissociation constant were observed during the washing step.

TA-PM, T-G SPM, T-T SPM, and T-C SPM, respectively. We report these preliminary results now; further study with different kinds of mismatches considering the nearest neighbors are under progress.

It is also worthwhile to note that the differences in dissociation constant are much more significant than those in the association constant. Therefore, one can conclude not only that the hybridization affinity is strongly dependent on the type of mismatches but also it might be even more important to have stringent washing conditions in order to have good sensitivity and selectivity for single-base-pair mutation detection.

#### 4. Summary

We have used QCM and fluorescence spectroscopy to characterize the immobilization of single-stranded DNA and the subsequence hybridization reactions with fully complementary or single-base mismatched sequences of DNA. As expected, the amount of DNA probe adsorbed increased when the salt concentration was high because of the reduced electrostatic repulsion between anionic DNA strands. Even though QCM is an indispensable tool for in situ monitoring of minute hybridization reactions on surfaces, the result can be affected by various factors for accurate surface density measurement due to an inherent mechanism. This weak point of the QCM measurement was compensated for as we adopted the fluorescence-based method and quantified the amount of DNA adsorbed. This could be also done with other experimental techniques such as ellipsometry, SPR, and XPS. The results showed that the surface density deduced from the frequency change in QCM measurement for the case of 1 M PBS was highly overestimated. Presumably this is due to the differences in conformation and viscoelastic properties of the adsorbed layer with hydrating buffer solution. Furthermore, the overestimation of the surface density was smaller for the double-stranded DNA than for the single-stranded DNA probe, which can be tentatively attributed to the structural differences. In addition, the hybridization experiments with single-base mismatched target DNA were conducted at various temperatures in order to find the hybridization temperature that gives the maximum discrimination capability. A preliminary study with SPR was conducted to investigate the binding affinities for different kinds of mismatched pairs. Depending on the type of single mismatched base pair, the dissociation constant was significantly varied.

#### Acknowledgments

We thank Dongkyu Jin for providing us the sequence of DNA samples and Taejoon Kwon for calculating the melting temperature of oligonucleotides using the nearest-neighbor model. This work was supported by the Ministry of Commerce, Industry and Energy (MOCIE) of the Republic of Korea under the a next generation new technology development project (00008069) through the Digital Bio Laboratory at the Samsung Advanced Institute of Technology (SAIT).

#### References

- [1] S.P.A. Fodor, Science 277 (1997) 393.
- [2] R.J. Lipshutz, S.P.A. Fodor, T.R. Gingeras, D.J. Lockhart, Nature Genetics Supplement 21 (1999) 20.
- [3] J. Fritz, M.K. Baller, H.P. Lang, H. Rothuizen, P. Vettiger, E. Meyer, H.-J. Güntherodt, Ch. Gerber, J.K. Gimzewski, Science 288 (2000) 316
- [4] C.A. Mirkin, R.L. Letsinger, R.C. Mucic, J.J. Storrhoff, Nature 382 (1996) 607.
- [5] G.P. Mitchell, C.A. Mirkin, R.L. Letsinger, J. Am. Chem. Soc. 121 (1999) 8122.
- [6] P.G. Schultz, Nature 382 (1996) 609.
- [7] E. Braun, Y. Eichen, U. Sivan, G. Ben-Yoseph, Nature 391 (1998) 775.
- [8] T.M. Herne, M.J. Tarlov, J. Am. Chem. Soc. 119 (1997) 8916.
- [9] A.B. Steel, T.M. Herne, M.J. Tarlov, Anal. Chem. 70 (1998) 4670.
- [10] A.B. Steel, R.L. Levicky, T.M. Herne, M.J. Tarlov, Biophys. J. 79 (2000) 975.
- [11] R. Levicky, T.M. Herne, M.J. Tarlov, S.K. Satija, J. Am. Chem. Soc. 120 (1998) 9787.
- [12] C. Bamdad, Biophys. J. 75 (1997) 1989.
- [13] C. Bamdad, Biophys. J. 75 (1997) 1997.
- [14] M. Satjapipat, R. Sanedrin, F. Zhou, Langmuir 17 (2001) 7637.
- [15] E. Huang, M. Satjapipat, S. Han, F. Zhou, Langmuir 17 (2001) 1215.
- [16] M. Sam, E.M. Boon, J.K. Barton, M.G. Hill, E.M. Spain, Langmuir 17 (2001) 5727.
- [17] K.A. Peterlinz, R.M. Georgiadis, T.M. Herne, M.J. Tarlov, J. Am. Chem. Soc. 119 (1997) 3401.
- [18] R. Georgiadis, K.P. Peterlinz, A.W. Peterson, J. Am. Chem. Soc. 122 (2000) 3166.
- [19] A.W. Peterson, R.J. Heaton, R. Georgiadis, J. Am. Chem. Soc. 122 (2000) 7837
- [20] J. Wang, P.E. Nielsen, M. Jiang, X. Cai, J. Roberto Fernandes, D.H. Grant, M. Ozsoz, A. Beglieter, M. Mowat, Anal. Chem. 69 (1997) 5200
- [21] F. Patolsky, A. Lichtenstein, I. Willner, J. Am. Chem. Soc. 122 (2000) 418
- [22] F. Caruso, E. Rodda, D.N. Furlong, K. Niikura, Y. Okahata, Anal. Chem. 1997 (1997) 2043.
- [23] Y. Okahata, Y. Matsunobu, K. Ijiro, M. Mukae, A. Murakami, K. Makino, J. Am. Chem. Soc. 114 (1992) 8299.

- [24] Y. Okahata, M. Kawase, K. Niikura, F. Ohtake, H. Furusawa, Y. Ebara, Anal. Chem. 70 (1998) 1288.
- [25] K. Niikura, H. Matsuno, Y. Okahata, J. Am. Chem. Soc. 120 (1998) 8537
- [26] J. Wang, M. Jiang, T.W. Nilsen, R.C. Getts, J. Am. Chem. Soc. 120 (1998) 8281.
- [27] F. Hook, A. Ray, B. Norden, B. Kasemo, Langmuir 17 (2001) 8305.
- [28] X.-C. Zhou, S.J. O'Shea, S.F.Y. Li, Chem. Commun. (2000) 953.
- [29] S. Han, J. Lin, M. Satjapipat, A.J. Baca, F. Zhou, Chem. Commun. (2001) 609.
- [30] T.H. Ha, K. Kim, Langmuir 17 (2001) 1999.

- [31] L.M. Demers, C.A. Mirkin, R.C. Mucic, R.A. Reynolds III, R.L. Letsinger, R. Elghanian, G. Viswanadham, Anal. Chem. 72 (2000) 5535
- [32] K. Hu, A.J. Bard, Langmuir 14 (1998) 4790.
- [33] Y.-K. Cho, S. Kim, G. Lim, S. Granick, Langmuir 17 (2001) 7732.
- [34] M.A.C. Plunkett, M. Per, M. Ernstsson, M.W. Rutland, Langmuir 19 (2003) 4673.
- [35] J. Santalucia, Proc. Natl. Acad. Sci. 95 (1998) 1460.
- [36] U.F. Jonsson, L. Ivarsson, B. Johnsson, B. Karlsson, R. Lundh, K. Lofas, S. Persson, B. Roos, H. Ronnberg, I. Sjolander, S. Stenberg, E. Stahlberg, R. Urbaniczky, C. Ostlin, H. Malmqvist, Biotechniques 11 (1991) 620.